

MAGNETAR SPINDOWN, HYPER-ENERGETIC SUPERNOVAE, & GAMMA RAY BURSTS

TODD A. THOMPSON^{1,2}, PHILIP CHANG³, & ELIOT QUATAERT⁴
SUBMITTED TO APJ: *January 23, 2004*

ABSTRACT

The Kelvin-Helmholtz cooling epoch, lasting tens of seconds after the birth of a neutron star in a successful core-collapse supernova, is accompanied by a neutrino-driven wind. For magnetar-strength ($\sim 10^{15}$ G) large scale surface magnetic fields, this outflow is magnetically-dominated during the entire cooling epoch. Because the strong magnetic field forces the wind to co-rotate with the protoneutron star, this outflow can significantly effect the neutron star's early angular momentum evolution, as in analogous models of stellar winds (e.g. Weber & Davis 1967). If the rotational energy is large in comparison with the supernova energy and the spindown timescale is short with respect to the time required for the supernova shockwave to traverse the stellar progenitor, the energy extracted may modify the supernova shock dynamics significantly. This effect is capable of producing hyper-energetic supernovae and, in some cases, provides conditions favorable for gamma ray bursts. We estimate spindown timescales for magnetized, rotating protoneutron stars and construct steady-state models of neutrino-magnetocentrifugally driven winds. We find that if magnetars are born rapidly rotating, with initial spin periods (P) of ~ 1 millisecond, that of order $10^{51} - 10^{52}$ erg of rotational energy can be extracted in ~ 10 seconds. If magnetars are born slowly rotating ($P \gtrsim 10$ ms) they can spin down to periods of ~ 1 second on the Kelvin-Helmholtz timescale.

Subject headings: stars: magnetic fields — stars: winds, outflows — stars: neutron — supernovae: general — gamma rays: bursts

1. INTRODUCTION

A successful supernova leaves behind a hot deleptonizing protoneutron star (PNS). This newly born, contracting, compact object radiates its gravitational binding energy in neutrinos, which ablate matter from its surface via energy deposition. The primary heating mechanisms are the charged-current processes of electron and anti-electron neutrino absorption on free nucleons: $\nu_e n \rightarrow pe^-$ and $\bar{\nu}_e p \rightarrow ne^+$. The neutrino energy (typically ~ 10 MeV) is deposited in the final-state leptons, which are hydrodynamically coupled to the nucleons. In this way, a thermal wind composed of nucleons and leptons is created. At the densities and temperatures surrounding the PNS at birth, photons are completely trapped and are advected with the wind (e.g. Duncan et al. 1986; Qian & Woosley 1996).

This neutrino-driven outflow emerges into the supernova post-shock environment – the supernova shock itself moving away from the protoneutron star at a velocity of 10-30,000 km s⁻¹ (e.g. Burrows, Hayes, & Fryxell 1995). The duration of the PNS wind is set by the cooling or Kelvin-Helmholtz timescale ($\tau_{KH} \sim GM^2/L_\nu R$, where L_ν is the total neutrino luminosity) for radiating away heat and lepton number and is typically of order tens of seconds (Burrows & Lattimer 1986; Pons et al. 1999). The kinetic luminosity of the wind is typically less than 10^{48} erg s⁻¹ and decreases sharply as the neutrino luminosity decreases (e.g. Qian & Woosley 1996) and the protoneutron star cools, and so the addition to the asymptotic supernova energetics is small on the scale of the canonical supernova energy, 10^{51} erg. Furthermore, the total mass ejected during the cooling epoch is

$\lesssim 10^{-3} M_\odot$, depending upon how the start of the wind phase is defined – minor in comparison with the total mass ejected in a typical core-collapse supernova. Despite this status as a mere perturbation to supernovae in both mass and energy, PNS winds have been the focus of considerable recent work. In particular, because of their intrinsic neutron-richness and association with supernovae, research on PNS winds has focused on the possibility that they might be the as yet unidentified astrophysical site for production of the r -process nuclides (Woosley et al. 1994; Takahashi et al. 1994; Qian & Woosley 1996; Cardall & Fuller 1997; Sumiyoshi et al. 2000; Otsuki et al. 2000; Wanajo et al. 2001; Thompson et al. 2001).

Recently, Thompson (2003a,b) noted that in the absence of rotation magnetar-like (e.g. Kouveliatou et al. 1999; Duncan & Thompson 1992; Thompson & Duncan 1993) surface magnetic field strengths ($B_0 \sim 10^{15}$ G) can dominate the thermal pressure and kinetic energy density of the wind in this very early phase of neutron star evolution. Here we extend this work by considering in a simplified model the combined action of neutrino heating, rotation, and strong magnetic fields.

Magnetic dipole radiation (e.g. Pacini 1967, 1968; Gunn & Ostriker 1969) and, to a lesser extent, gravitational wave radiation (e.g. Ostriker & Gunn 1969) are often considered as dominant spindown mechanisms, controlling the rate of rotational energy extraction and the angular momentum evolution of young neutron stars. Here we consider a mechanism well-known to the solar physics community: magnetic braking by the combined action of a persistent outflow and a strong magnetic field (Weber & Davis 1967; Mestel 1968; Belcher & Mac-

¹ Hubble Fellow² Astronomy Department and Theoretical Astrophysics Center, 601 Campbell Hall, University of California, Berkeley, CA 94720; thomp@astro.berkeley.edu³ Department of Physics, Broida Hall, University of California, Santa Barbara, CA 93106; pchang@physics.ucsb.edu⁴ Astronomy Department and Theoretical Astrophysics Center, 601 Campbell Hall, University of California, Berkeley, CA 94720; eliot@astro.berkeley.edu

gregor 1976; Hartmann & Macgregor 1982; Mestel & Spruit 1987). For a wide range of initial rotation periods, we find that protoneutron stars may be spun down by the presence of this neutrino-magnetocentrifugally driven outflow in the first tens of seconds of the PNS's life. If these highly magnetic objects are born rapidly rotating, $\sim 10^{52}$ erg may be extracted on the cooling timescale, giving an energetic boost to the just-preceding supernova and providing favorable conditions for gamma ray bursts.

Although our focus is on magnetars born with millisecond periods, we also assess the evolution of highly magnetic objects born slowly rotating, with spin periods similar to those of radio pulsars (tens to hundreds of milliseconds). Our conclusions for these objects are sensitively dependent upon magnetic field geometry. However, for monopole-like fields we come to the interesting conclusions that these objects are spun down considerably on the cooling timescale; a PNS with ~ 20 ms initial period is transformed into a ~ 1 second rotator in τ_{KH} .

1.1. This Paper

In §2 we review the basics of stellar spindown via magnetocentrifugal outflows and provide some motivation for pursuing this effect in PNS winds. Section 3 discusses some aspects and ambiguities of the expected magnetic field topology. In §4 we provide simple analytic scalings for the Alfvén point and spindown timescales over a wide range of initial PNS spin periods. Section 5 describes our models of neutrino-magnetocentrifugally-driven outflows and presents estimates of rotational energy extraction. In §6 we discuss applications to hypernovae and gamma ray bursts, making contact with Usov (1992) and Thompson (1994). We further summarize our findings, review the potential implications for supernova remnants and the angular momentum evolution of young neutron stars, and highlight open questions in need of further investigation. Throughout this paper we refer to models of non-rotating, non-magnetic PNS winds (e.g. the models of Duncan et al. 1986; Takahashi et al. 1994; Qian & Woosley 1996; Sumiyoshi et al. 2000; Otsuki et al. 2000; Wanajo et al. 2001; Thompson et al. 2001) with the acronym ‘NRNM’.

2. SPINDOWN

Mass loss from the surface of any rotating star carries away angular momentum. If the star has a strong magnetic field, the matter lost in the stellar wind is forced into near corotation with the stellar surface out to $\sim R_A$, the Alfvén point, where the magnetic energy density equals the kinetic energy density of the outflow. This effect provides for efficient angular momentum transport from the rotating star to the outflow (Schatzman 1962). Angular momentum conservation implies that

$$\frac{d}{dt}(I\Omega) = -\dot{M}\mathcal{L} \quad (1)$$

where I is the moment of inertia, Ω is the angular velocity at the stellar surface, \dot{M} is the wind mass loss rate, and \mathcal{L} is the specific angular momentum carried by the wind. In the classic model for solar spindown constructed by Weber & Davis (1967), the problem is treated in one spatial dimension at the equator with $\mathbf{B} = B_r\hat{\mathbf{e}}_r + B_\phi\hat{\mathbf{e}}_\phi$ and $\mathbf{v} = v_r\hat{\mathbf{e}}_r + v_\phi\hat{\mathbf{e}}_\phi$. At the stellar

surface $B_r \gg B_\phi$, and the field is monopolar, $B_r \propto r^{-2}$.⁵ Consideration of the azimuthal momentum equation together with Faraday's law yields

$$\mathcal{L} = rv_\phi - \left(\frac{rB_r B_\phi}{4\pi\rho v_r} \right) = \text{constant} = R_A^2 \Omega, \quad (2)$$

where ρ is the mass density. Although the magnetic field lines bend in the $-\phi$ direction between the stellar surface and R_A , such that $B_r(R_A) \sim B_\phi(R_A)$, eq. (2) states that the wind has angular momentum as if strict co-rotation is enforced between the magnetic field footpoints and R_A .

Employing eq. (2) in eq. (1) and taking $I = (2/5)MR_\nu^2$, where M is the PNS mass and R_ν is the PNS radius⁶, one finds that

$$\Omega_f = \Omega_i (M_f/M_i)^{\frac{5}{2}(R_A/R_\nu)^2}. \quad (3)$$

Here we have assumed that R_ν and R_A are independent of time. The subscripts f and i denote ‘final’ and ‘initial’, respectively. In the absence of magnetic fields, $R_A = R_\nu$ and for a total mass loss of even $10^{-2} M_\odot$, Ω changes by just 1% for a solar mass neutron star. For strong magnetic fields, however, we expect a large R_A/R_ν , and, correspondingly, large $\Delta\Omega$. If strongly magnetized PNSs are born rapidly rotating (Duncan & Thompson 1992; Thompson & Duncan 1993) then a reservoir of rotational energy,

$$E_{\text{Rot}} = \frac{1}{2}I\Omega^2 \sim \frac{1}{5}MR_\nu^2\Omega^2 \simeq 2.2 \times 10^{52} \text{ erg } M_{1.4} R_{\nu 10}^2 P_1^{-2}, \quad (4)$$

large in comparison with 10^{51} erg, may be extracted on the spindown timescale. In eq. (4), $M_{1.4} = M/1.4 M_\odot$, $R_{\nu 10} = R_\nu/10$ km, and P_1 is the spin period in units of 1 millisecond (ms). The spindown timescale is defined here as the e -folding time for Ω (combining eqs. 1 and 2);

$$\tau_J = \frac{\Omega}{\dot{\Omega}} = \frac{2M}{5\dot{M}} \left(\frac{R_\nu}{R_A} \right)^2. \quad (5)$$

If τ_J is short compared with the Kelvin-Helmholtz cooling timescale for the PNS, then the angular momentum of the PNS is significantly effected during the wind epoch. Also, because E_{Rot} is potentially much larger than 10^{51} erg, if τ_J is short compared with the time for the just-preceding supernova shockwave to traverse the progenitor, then we expect interesting observational consequences and modifications to the supernova explosion, resulting nucleosynthesis, and remnant dynamics. The last of these, that the supernova remnant may have larger inferred asymptotic kinetic energy is not unique to this spindown mechanism. Simple vacuum dipole spindown also energizes the supernova remnant on a *relatively* short timescale for highly magnetic, rapidly rotating neutron stars. The primary differences here is that if a large fraction of the rotational energy can be tapped quickly, the nucleosynthesis of the actual explosion can be modified. This difference is of particular importance because, as we show in §4, the spindown timescale given in eq. (5) can be significantly shorter than that inferred from vacuum dipole spindown.

3. FIELD TOPOLOGY

To calculate the spindown of PNSs, we must estimate R_A . To do so, we appeal to its definition – the point at which the

⁵ This field configuration is often referred to as ‘split-monopole’.

⁶ The subscript ν refers to the fact that in the PNS case we take the ‘surface’ to correspond to the radius of neutrino decoupling, the neutrino-sphere.

magnetic energy density ($B^2/8\pi$) equals the radial wind kinetic energy density ($\rho v_r^2/2$). For the purposes of simplicity and generality, we take

$$B_r = B_0(R_\nu/r)^\eta. \quad (6)$$

The Weber-Davis model posits a monopole field structure with $\eta = 2$. With this dependence of B on r , we may estimate R_A and τ_J . We may rightly ask, however, whether or not these estimates are appropriate considering the fact that the currents in the star should necessarily produce – to lowest order – a dipole field with $\eta = 3$. This question is germane because the predicted R_A is much smaller if one assumes a dipole field and, consequently, the inferred τ_J is much longer. The ambiguity is due to the intrinsically multi-dimensional nature of magnetically-dominated outflows. Analytical (e.g. Mestel 1968; Mestel & Spruit 1987) and numerical models (e.g. Pneumann & Kopp 1971; Steinolfson et al. 1982; Usmanov et al. 2000; Lionello et al. 2002; Ud-Doula & Owocki 2002) show that the interaction between the magnetic field and the flow is complex. The steady-state structure, for modestly magnetically-dominated flows, is the classic helmet-streamer configuration (see Fig. 1 of Mestel & Spruit 1987 for a depiction) with magnetic field lines emerging from low latitudes forming a ‘dead zone’, a region of closed magnetic loops, and the wind at high latitudes opening the field to infinity. The resulting field is a mix of ‘monopole’ and ‘dipole’.

Because the kinetic energy density of the outflow dominates the magnetic field for $r > R_A$, and vice-versa for $r < R_A$, one might naively expect that inside R_A the field is roughly dipolar and outside R_A it is monopolar. This picture is the most conservative from the point of view of spindown and describes the basics of the model of Mestel (1968). Rapid rotation complicates the issue. Mestel & Spruit (1987) show that the radial extent of the dipolar region, the dead zone (R_D), can be smaller than R_A (also implied by Ud-Doula 2002). Assuming isothermal conditions, the radial extent of the dead zone can be calculated from the equations of magnetohydrostatic equilibrium;

$$\left(\frac{R_\nu}{R_D}\right)^6 = \frac{\rho_\nu c_{T_\nu}^2}{(B_0^2/8\pi)} \exp\left[-\frac{GM}{R_\nu c_{T_\nu}^2} \left(1 - \frac{R_\nu}{R_D}\right)\right] \times \exp\left[\frac{R_\nu^2 \Omega^2}{2c_{T_\nu}^2} \left(\frac{R_D^2}{R_\nu^2} - \frac{R_\nu}{R_D}\right)\right] \quad (7)$$

where c_{T_ν} and ρ_ν denote the isothermal sound speed and mass density, respectively, in the dead zone, at R_ν . Equation (7) is a consequence of balancing magnetic tension with thermal pressure in an isothermal magnetohydrostatic atmosphere. Taking fiducial PNS parameters as in §4 ($R_\nu = 10$ km, $P = 1$ ms, $B_0 = 10^{15}$ G, and $M = 1.4 M_\odot$), R_D is typically < 20 km, depending upon the choice for ρ_ν and c_{T_ν} , much less than R_A (see eq. 10). In the range of radii $R_D < r < R_A$, the field lines are opened into a monopole configuration and R_A is estimated with $\eta = 2$ for the field structure. This effect yields spindown timescales that are shorter than those inferred from the more pessimistic case in which a dipole is assumed from the stellar surface all the way out to R_A . Therefore, eq. (7) implies that for rapid rotation (where ‘rapid’ is defined by the ratio $R_\nu^2 \Omega^2 / c_{T_\nu}^2$) the net spindown might be better approximated by employing a pure monopole model, whereas for slow rotation a dipole field is probably more appropriate.

In addition to this centrifugal effect, there are several other reasons to suspect that in estimating R_A we should take $\eta < 3$

in eq. (6). First, any net twist to the magnetic field lines yields $\eta < 3$ and spindown is enhanced (Thompson et al. 2001). Second, the braking indices inferred from observations of pulsars, a system in which the pure dipole limit should strictly obtain, are inconsistent with $\eta = 3$. Third, the dead zone on the surface of a PNS may be periodically opened by neutrino heating (Thompson 2003), footpoint motion and shear (Thompson & Murray 2001), or MHD instabilities. In short, η must be less than 3, but it is greater than 2. Both are limiting cases. The complications of rapid rotation (eq. 7), relativity (we encounter relativistic outflows in §4), and neutrino heating make this ambiguity resolvable only with multi-dimensional numerical simulations of thermal magnetocentrifugal winds.

In what follows, we present estimates for arbitrary η and scalings for $\eta = 2$ and $\eta = 3$. As we have just argued, our results for the monopole case likely over-estimate the efficacy of spindown (Poe, Friend, & Cassinelli 1989; Keppens & Goedbloed 1999; Van der Holst et al. 2002; *but*, see Pizzo et al. 1983). However, the results from the pure dipole ($\eta = 3$) limit must under-estimate spindown (Mestel & Spruit 1987).

4. ESTIMATES

At R_A , $B^2/8\pi \sim \rho v_r^2/2$. With eq. (6), and using $\rho = \dot{M}/4\pi r^2 v_r$,

$$R_A^{2\eta-2} = B_0^2 R_\nu^{2\eta} \dot{M}^{-1} v_A^{-1}, \quad (8)$$

where $v_A = v_r(R_A)$ is the Alfvén speed. Let v_ν denote the asymptotic velocity attained by the matter in a purely NRM outflow (that is, in a wind with $\Omega = 0$ and $B_0 = 0$). Because the flow in NRM wind models is driven by extremely inefficient neutrino heating, v_ν is typically much less than the PNS escape speed (see e.g. Thompson et al. 2001). For high neutrino luminosity $v_\nu \lesssim 3 \times 10^9$ cm s⁻¹. If the matter is forced to co-rotate to $\sim R_A$, then $v_\phi(R_A) \sim R_A \Omega$. If $R_A \Omega \gtrsim v_\nu$ we expect that $v_r(R_A) \sim v_\phi(R_A)$. These arguments imply that to reasonable approximation $v_A \sim R_A \Omega$. Therefore, from eq. (8),

$$R_A^{2\eta-1} = B_0^2 R_\nu^{2\eta} \dot{M}^{-1} \Omega^{-1}. \quad (9)$$

Scaling for a rapidly rotating magnetar ($P = 1$ ms),

$$R_A(\eta = 2) \simeq 43 \text{ km } B_{0,15}^{2/3} R_{\nu,10}^{4/3} \dot{M}_{-3}^{-1/3} P_1^{1/3} \quad (10)$$

$$R_A(\eta = 3) \simeq 24 \text{ km } B_{0,15}^{2/5} R_{\nu,10}^{6/5} \dot{M}_{-3}^{-1/5} P_1^{1/5} \quad (11)$$

Here and throughout this paper, $B_{0,n} = B_0/10^n$ G, $\dot{M}_{-m} = \dot{M}/10^{-m} M_\odot$ s⁻¹, and $P_l = P/l$ ms. Note that these scalings apply only when the condition $R_A \Omega \gtrsim v_\nu$ is satisfied.⁸

There are several features of winds from rapidly rotating magnetically-dominated PNSs that are very different from their NRM counterparts. Specifically, for the estimate given for R_A in eq. (9) to apply, R_A must be greater than R_{sonic} , the sonic point, where the radial velocity is equal to the local adiabatic sound speed (c_s). However, typical NRM models yield R_{sonic} in the range of hundreds of kilometers, much larger than R_A as implied by eqs. (10) and (11). This apparent problem is reconciled easily; in highly magnetic, rapidly rotating PNS winds, R_{sonic} occurs at radii much smaller than those inferred from NRM models. The boundary conditions at the PNS surface

⁷ This is equivalent to assuming the *fast magnetic rotator* (FMR) limit of Belcher & Macgregor (1976).

⁸ In the more general case ($v_\nu \sim R_A \Omega$), one might take $v_A \sim (v_\nu^2 + R_A^2 \Omega^2)^{1/2}$ in eq. (8). For comparison, Taam & Spruit (1989) employ $v_A \sim [v_\nu^2 + (8/27)R_A^2 \Omega^2]^{1/2}$.

– that the neutrinos are in thermal and chemical equilibrium with the matter and that the neutrino optical depth is $\sim 2/3$ (see Thompson et al. 2001) – conspire to give a sound speed (c_s) at R_ν of $\sim 3 \times 10^9$ cm s $^{-1}$. Therefore, for $R_\nu = 10$ km and spin period shorter than ~ 2 ms ($\Omega \gtrsim 3000$ rad s $^{-1}$) $R_\nu \Omega$ exceeds $c_s(R_\nu)$. This limit, $v_\phi(R_\nu) \gg c_s(R_\nu)$, is termed ‘centrifugal’ (Lamers & Cassinelli 1999). In this limit, the centrifugal force dominates wind driving and we may neglect both neutrino heating and the gas pressure in the critical wind equations near R_{sonic} (see e.g. eq. 25; discussion of the general wind equations is deferred to §5). A simple expression results;

$$v_e^2/2|_{R_{\text{sonic}}} = v_\phi^2|_{R_{\text{sonic}}}, \quad (12)$$

where v_e is the local escape velocity. The location of the sonic point is then

$$R_{\text{sonic}} = (GM/\Omega^2)^{1/3} = (R_{\text{Sch}} R_L^2/2)^{1/3} \simeq 16.8 \text{ km } M_{1.4}^{1/3} P_1^{-2/3}, \quad (13)$$

where R_{Sch} is the Schwarzschild radius (~ 4.15 km for a 1.4 M_\odot PNS). With this estimate we find that the sonic point occurs much closer to the PNS and that $R_A > R_{\text{sonic}}$ for eqs. (10) and (11).

There is another feature of centrifugal winds that differs significantly from NRNM outflows. As $R_\nu \Omega$ becomes greater than $c_s(R_\nu)$ the matter density scale height increases exponentially with Ω^2 due to centrifugal support in the near-hydrostatic region ($v_r \ll c_s$). For this reason, the derived mass loss rate also increases exponentially with Ω^2 . Note that this is only true if the magnetic field supports the flow from the surface of the star to the sonic point. That is, we only expect large increases in \dot{M} for $R_A \geq R_{\text{sonic}}$. Examining eq. (5) we see that with \dot{M} increasing exponentially with Ω^2 , τ_J may become very short for large Ω . However, as Ω is increased and the mass loading on the field lines increases, B_0 must be large enough to guarantee $R_A > R_{\text{sonic}}$ (eq. 9). In NRNM models, characteristic mass loss rates are less than $10^{-4} M_\odot$ s $^{-1}$. The exponential effect on \dot{M} in the centrifugal limit justifies our use of a much higher mass loss rate in eqs. (10) and (11), when $P = 1$ ms (see Fig. 2 and §5).

In an effort to make contact with the pulsar and solar wind communities, it is worth noting that taking eq. (9) and multiplying both sides by Ω^3 for $\eta = 2$, one obtains

$$v_A^3 = v_M^3 \equiv \frac{\Omega^2 B_0^2 R_\nu^4}{\dot{M}} = \frac{\Omega^2 F_B}{F_M}, \quad (14)$$

where F_B is the magnetic flux, F_M is the matter flux, and v_M is the Michel velocity (Michel 1969; Belcher & Macgregor 1976). As one would expect from the Bernoulli integral, it is the Michel velocity that, to constants of order unity, is the asymptotic wind velocity. In a true fast ($v_\nu \ll R_A \Omega$), magnetically dominated wind the Alfvén velocity is 2/3 of the Michel velocity, and v_M obtains only at the fast magnetosonic point (e.g. Belcher & MacGregor 1976). In fact, for a strictly monopolar cold ($c_s = 0$ everywhere) magnetocentrifugal wind the fast point is formally at infinity (Michel 1969). At the level of accuracy aspired to here, these details are unimportant.

Spindown timescales ($\tau_J = \Omega/\dot{\Omega}$; eq. 5) can be computed from the estimates of R_A in eqs. (10) and (11). Together with eq. (9) we find that

$$\tau_J^{\text{NR}} = (2/5) M \dot{M}^{(3-2\eta)/(2\eta-1)} R_\nu^{-2/(2\eta-1)} B_0^{-4/(2\eta-1)} \Omega^{2/(2\eta-1)}. \quad (15)$$

The superscript ‘NR’ is added to emphasize that when the flow is non-relativistic, τ_J depends explicitly on \dot{M} as in eq. (5). For relativistic flows it does not (see eq. 22). Taking $M = 1.4 M_\odot$ and scaling,

$$\tau_J^{\text{NR}}(\eta = 2) \simeq 30 \text{ s } M_{1.4} \dot{M}_3^{-1/3} R_{\nu 10}^{-2/3} B_{015}^{-4/3} P_1^{-2/3} \quad (16)$$

$$\tau_J^{\text{NR}}(\eta = 3) \simeq 96 \text{ s } M_{1.4} \dot{M}_3^{-3/5} R_{\nu 10}^{-2/5} B_{015}^{-4/5} P_1^{-2/5} \quad (17)$$

The important timescale to compare with τ_J^{NR} is the Kelvin-Helmholtz cooling timescale, τ_{KH} . This comparison is relevant because \dot{M} drops steeply with the PNS neutrino luminosity. If $\tau_J^{\text{NR}} \gg \tau_{\text{KH}}$ no spindown occurs during the wind epoch. The PNS cooling calculations of Pons et al. (1999) show that L_ν^{tot} drops by a factor of ten, from $\sim 10^{52}$ erg s $^{-1}$ to $\sim 10^{51}$ erg s $^{-1}$, in ~ 30 seconds. This result depends on the mass of the PNS and the high-density nuclear equation of state employed. These calculations do not include the effects of rapid rotation or high magnetic fields. Both may significantly modify τ_{KH} . Rapid rotation leads to lower core temperatures and, thereby, lower average neutrino luminosity. This could increase τ_{KH} significantly (see Thompson, Quataert, & Burrows, in prep; Yuan & Heyl 2003; Villain et al. 2003). Rapid rotation might also make R_ν contract more slowly, affecting both B_0 and Ω at a given time because both are proportional to R_ν^{-2} , via flux and angular momentum conservation, respectively. High B_0 may also affect τ_{KH} by modifying neutrino opacities (e.g. Lai & Qian 1998; Arras & Lai 1999). Multi-dimensional effects such as convection may also be important (Keil, Janka, & Müller 1996). Without detailed models of magnetar cooling, we take the results of Pons et al. (1999) as representative and define $\tau_{\text{KH}} \sim 30$ seconds.

As argued in §3 the spindown timescales relative to τ_{KH} are sensitive both in absolute value and scaling to the parameter η . Even allowing for our ignorance about the magnetic field topology, eqs. (16) and (17) imply that at best $\tau_J^{\text{NR}} \sim \tau_{\text{KH}}$ for the PNS parameters chosen. Note that for higher \dot{M} , both timescales decrease somewhat, despite the fact that R_A decreases as \dot{M} increases. Interestingly, for larger initial spin periods, the spindown timescales *decrease*. Hence, if magnetars are born with $P \sim 30$ ms – consistent with the spin periods of most pulsars today – then $\tau_J^{\text{NR}} \sim 3$ s and ~ 25 s for $\eta = 2$ and $\eta = 3$, respectively. As we will see in §5 mass loss rates as high as $10^{-3} M_\odot$ s $^{-1}$ are probably unrealistic at such low Ω . Even so, spindown of slowly rotating magnetars during the cooling epoch can be quite efficient. For higher B_0 , both spindown timescales drop rapidly. Increasing the surface magnetic field strength to 10^{16} G in eq. (17), $\tau_J^{\text{NR}}(\eta = 3) \simeq 15$ s, which may be considerably less than τ_{KH} . Although such a large B_0 is not out of the question in this very early phase of PNS evolution, it is well beyond the surface field strengths inferred from magnetars (Kouveliotou et al. 1999; Thompson & Duncan 1993).

Consideration of such high field strengths brings up an important physical constraint on R_A , particularly germane for PNSs rotating rapidly at birth: R_A cannot be made arbitrarily large by increasing B_0 for a given Ω because v_ϕ would eventually exceed the speed of light. Thus, the Alfvén point, determined *a posteriori* for a given Ω , must be less than the light cylinder radius, $R_L = c/\Omega$, although for asymptotically large ratios of magnetic flux to matter flux R_A asymptotes to R_L . This requirement sets a critical B_0 . If we set $R_A = R_L = c/\Omega$ in eq. (9) for a given Ω , R_ν , and \dot{M} , the B_0 derived is that required to enforce co-rotation to *approximately* R_L . This critical magnetic

field, for arbitrary η , is easily derived in terms of the basic wind and PNS parameters;

$$B_{\text{crit}} = c^{(2\eta-1)/2} \dot{M}^{1/2} \Omega^{1-\eta} R_\nu^{-\eta}. \quad (18)$$

For example, for a neutron star with spin period of 1 ms, $R_L \simeq 47.7$ km and for $\dot{M} = 10^{-3} M_\odot \text{ s}^{-1}$ as in eqs. (16) and (17), $B_{\text{crit}} \simeq 1.2 \times 10^{15}$ G and 5.7×10^{15} G for $\eta = 2$ and $\eta = 3$, respectively.

If R_A is sufficiently less than R_L , the asymptotic velocity of the wind material is not relativistic. In non-relativistic outflows, consideration of the Bernoulli integral in the Weber-Davis model shows that the energy carried by the magnetic field is a factor of two greater than that of the matter (e.g. Lamers & Cassinelli 1999) and the rotational energy loss rate is

$$\dot{E}_{\text{tot}} = I\Omega\dot{\Omega} = -\dot{M}\mathcal{L}\Omega = -B_0^{4\zeta} R_\nu^{4\eta\zeta} \dot{M}^{1-2\zeta} \Omega^{2-2\zeta}, \quad (19)$$

where $\zeta = 1/(2\eta - 1)$. If B_0 exceeds B_{crit} , R_A approaches R_L and v_A approaches c . The flow becomes relativistic and the field may carry more than two times the energy of the matter. At R_L , the ratio of magnetic flux to matter flux is given by⁹

$$\Gamma = \frac{B^2}{4\pi\rho c^2} \Big|_{R_L} = B_0^2 R_\nu^{2\eta} \Omega^{2\eta-2} c^{1-2\eta} \dot{M}^{-1}. \quad (20)$$

and the relativistic energy loss rate is

$$\dot{E}_{\text{tot}} = -\Gamma \dot{M} c^2 = -B_0^2 R_\nu^{2\eta} \Omega^{2\eta-2} c^{3-2\eta}. \quad (21)$$

Note that \dot{E}_{tot} is independent of \dot{M} , but depends on the magnetic field structure. For the case $\eta = 3$, the pure magnetic vacuum dipole scaling for \dot{E}_{tot} is obtained.¹⁰ For $\eta = 2$, this expression for \dot{E}_{tot} implies a much larger energy loss rate than for $\eta = 3$ – the ratio being $c^2/R_\nu^2\Omega^2$, a factor of ~ 23 for a 10 km PNS with a 1 ms spin period. As \dot{M} drops during the cooling epoch, for constant B_0 , the wind transitions from a non-relativistic (eq. 19) to a relativistic outflow (eq. 21). Only in the case where Ω is very small so that R_L is very large are there instances when the wind is always non-relativistic during τ_{KH} (see §5.3). Taking eq. (20), the spindown timescale ($\tau_J = \Omega/\dot{\Omega}$) for relativistic winds, in analogy with eq. (15), is

$$\tau_J^{\text{R}} = (2/5) M R_\nu^{2-2\eta} B_0^{-2} \Omega^{4-2\eta} c^{2\eta-3}. \quad (22)$$

Taking the same scalings as in eqs. (16) and (17)

$$\tau_J^{\text{R}}(\eta = 2) \simeq 34 \text{ s } M_{1.4} R_{\nu_{10}}^{-2} B_{0.15}^{-2} \quad (23)$$

$$\tau_J^{\text{R}}(\eta = 3) \simeq 760 \text{ s } M_{1.4} R_{\nu_{10}}^{-4} B_{0.15}^{-2} P_1^2 \quad (24)$$

The superscript ‘R’ is meant to reinforce the difference between relativistic and non-relativistic wind spindown – the latter depending explicitly on \dot{M} . Comparing eqs. (24) and (17) we see that τ_J^{NR} is significantly shorter than τ_J^{R} . The difference is one of applicability. Equation (17) applies with large \dot{M} , when $R_A < R_L$ and $\Gamma < 1$. Equation (24) applies only when the mass flux from the PNS subsides to such an extent that $\Gamma \geq 1$. Taking $B_0 = B_{\text{crit}}$ in eq. (17), $\tau_J^{\text{NR}} = \tau_J^{\text{R}}$. Therefore, application of vacuum dipole spindown is appropriate only when \dot{M} is sufficiently small. We see that a naive and inappropriate application

⁹ The ratio Γ , as defined in eq. (20), is often denoted by ‘ σ ’ in the pulsar literature.

¹⁰ Note that in the standard theory (see e.g. Shapiro & Teukolsky 1983 chapter 10 for a review) \dot{E}_{tot} in the vacuum dipole limit includes a factor $\sin^2 \alpha/6$, where α is the angle between the spin axis of the neutron star and its magnetic axis.

¹¹ Although both considered magnetars in the context of soft gamma repeaters and anomalous X-ray pulsars, Thompson & Blaes (1998) and Harding et al. (1999) showed that enhanced spindown is obtained in models including relativistic particle winds.

¹² We have developed a one-dimensional non-relativistic time-dependent Eulerian magnetohydrodynamics code for solving the isothermal Weber-Davis problem. Preliminary comparisons between models in which strict corotation is enforced ($v_\phi = r\Omega$) everywhere and the actual Weber-Davis solution show that R_A is typically ~ 1.5 times larger than that expected from the models presented here. This implies that we underestimate the magnitude of the spindown for a given B_0 and overestimate spindown timescales τ_J^{NR} by a factor of ~ 2 .

of eq. (24) when the mass flux is $\sim 10^{-3} M_\odot \text{ s}^{-1}$ under-predicts the rate of angular momentum loss by a factor of ~ 8 .¹¹ Note that this discrepancy is much larger for slowly rotating magnetars; $\tau_J^{\text{R}}(\eta = 3)/\tau_J^{\text{NR}}(\eta = 3) \propto P^{12/5}$. If magnetars are born with $P = 10$ ms, $\tau_J^{\text{R}}/\tau_J^{\text{NR}} \sim 2000$ and one may under-predict spindown by several orders of magnitude. Of course, the difference is further magnified if, when the mass loss rate is high, the field is monopolar to some extent, as argued in §3. In this case we compare eq. (24) ($\eta = 3$) with eq. (16) ($\eta = 2$) and find that the vacuum dipole limit overestimates the spindown timescale by a factor of ~ 25 for the fiducial 1 ms rotator with $B_0 = 10^{15}$ G. Noting that $\tau_J^{\text{R}}(\eta = 3)/\tau_J^{\text{NR}}(\eta = 2) \propto P^{8/3}$, we see that this ratio is $\sim 10^4$ for a slow rotator with $P = 10$ ms.

5. NEUTRINO-MAGNETOCENTRIFUGAL WINDS ON THE CHEAP

Because the spindown timescales and the amount of rotational energy extractable depend so crucially on \dot{M} , we solve here the steady-state wind equations including neutrino heating and rotation explicitly. Magnetic fields are included implicitly by enforcing $v_\phi = r\Omega$ everywhere. Thus, the wind mass elements are forced to corotate with the PNS surface as if on wires emanating radially from the equator of the PNS like the spokes on a bike wheel. This approximates the effect of a strong magnetic field or the non-relativistic Weber-Davis problem. Of course, in our solution the mass elements eventually have velocity greater than c . For a given Ω , the radius at which this occurs is the light cylinder. For this reason our solutions are valid (if approximately) only for $r < R_L$. Importantly, since it is the effect of the centrifugal force on \dot{M} that we are most interested in, and \dot{M} will be most effected by the centrifugal force in the subsonic region, the sonic point (see eq. 13) is always well within R_L where the corotation assumption is valid.

It would be preferable to solve the one-dimensional relativistic Weber-Davis problem (Michel 1969; Goldreich & Julian 1970) with an arbitrary energy deposition function. We save this for a future paper.¹² Much more important, we feel, is our assumption that the problem may be treated in one spatial dimension (as in Weber & Davis 1967) in the presence of rapid rotation and strong magnetic fields (see §3). This approximation, can only be removed with a code capable of two-dimensional axisymmetric relativistic MHD for $\beta \ll 1$. This is a considerable effort beyond the scope of the current work.

5.1. Equations

Enforcing continuity, conservation of momentum, and conservation of energy in Newtonian gravity, we have that

$$\frac{1}{v_r} \frac{dv_r}{dr} (c_s^2 - v_r^2) = \frac{2}{r} \left(\frac{v_e^2}{4} - \frac{v_\phi^2}{2} - c_s^2 \right) + \dot{q} \frac{D}{C_V T v_r} \quad (25)$$

$$\frac{1}{\rho} \frac{d\rho}{dr} (c_s^2 - v_r^2) = \frac{2}{r} \left(v_r^2 - \frac{v_e^2}{4} + \frac{v_\phi^2}{2} \right) - \dot{q} \frac{D}{C_V T v_r} \quad (26)$$

$$\frac{D}{T} \frac{dT}{dr} \left(\frac{c_s^2 - v_r^2}{c_s^2 - c_T^2} \right) = \frac{2}{r} \left(v_r^2 - \frac{v_e^2}{4} + \frac{v_\phi^2}{2} \right) + \dot{q} \frac{D}{C_V T v_r} \left(\frac{c_T^2 - v^2}{c_s^2 - c_T^2} \right), \quad (27)$$

where $v_e = (2GM/r)^{1/2}$, $D = (T/\rho)\partial P/\partial T|_\rho$, c_T and c_s are the isothermal and adiabatic sound speeds, respectively, C_V is the specific heat at constant volume, $v_\phi = r\Omega$, v_r is the radial velocity, and \dot{q} is the specific neutrino heating rate. For a given Ω , we solve the above equations for the flow between the surface of the PNS and the sonic point as a two-point boundary value problem, using a relaxation algorithm, on an adaptive radial mesh (see Thompson et al. 2001). We integrate from the sonic point to the light cylinder using a simple Runge-Kutta algorithm. The equation of state (EOS) assumes ideal nucleons. It includes a general electron-positron EOS, photons, and neglects the formation of alpha particles. Magnetic effects on the EOS, particularly important for electron-positron component at low temperatures, have not been included. Once a solution is obtained, we can see what surface magnetic field strength is required to corotate out to any radius. Once the field is chosen, the solution is valid only inside this *a posteriori*-posited Alfvén point. Outside this radius, our solutions continue to accelerate as a result of the centrifugal force. In the full Weber-Davis problem, v_ϕ begins to decrease at R_A and v_r asymptotes, reaching the Michel velocity at the fast magnetosonic point (see Belcher & Macgregor 1976).

5.2. NMC Wind Results

Figure 1 shows the thermal pressure (solid line) and kinetic energy density ($\rho v_\phi^2/2$ long dashed line and $\rho v_r^2/2$ short dashed line) for a PNS with $L_{\bar{\nu}_e} = 4 \times 10^{51}$ erg s $^{-1}$, $M = 1.4 M_\odot$, and $R_\nu = 10$ km. We use $L_{\bar{\nu}_e}$ to label wind models; the total neutrino luminosity for a given model is $L_\nu^{\text{tot}} = L_{\nu_e} + L_{\bar{\nu}_e} + 4L_{\nu_\mu}$, with $L_{\nu_e} = L_{\bar{\nu}_e}/1.3$ and $L_{\nu_\mu} = L_{\bar{\nu}_e}/1.4$. The subscript ‘ ν_μ ’ stands for ν_μ , $\bar{\nu}_\mu$, ν_τ , and $\bar{\nu}_\tau$. For $L_{\bar{\nu}_e} = 4 \times 10^{51}$ erg s $^{-1}$, $L_\nu^{\text{tot}} \simeq 1.85 \times 10^{52}$ erg s $^{-1}$. The PNS period is taken to be 1 ms ($\Omega = 6283$ rad s $^{-1}$). Overlaid on Fig. 1 is the magnetic energy density (dotted lines, labeled $B^2/8\pi$) for $\eta = 2$ and $\eta = 3$ such that $B^2/8\pi \sim \rho c^2/2$ at R_L . The point at which the dotted curves intersect the short dashed lines corresponds to the Alfvén radius. The surface magnetic field strengths are labeled B_0 and correspond to B_{crit} in eq. (18) for $\eta = 2$ and $\eta = 3$. For these field strengths, then, the Alfvén point corresponds to $\sim R_L$. For lower B_0 , R_A decreases. Figure 1 shows that we can expect a 1.6×10^{15} G surface magnetic field with monopolar field topology to enforce corotation out to $\sim R_L$ for mass loss rates in the range of $10^{-3} M_\odot$ s $^{-1}$ (the model shown has $\dot{M} \simeq 1.6 \times 10^{-3} M_\odot$ s $^{-1}$). For $\eta = 3$, the required surface field strength is $\sim 7.5 \times 10^{15}$ G. As L_ν^{tot} increases \dot{M} increases and larger B_0 is required to force corotation out to R_L . As L_ν^{tot} decreases, the converse is true. For example, for $L_{\bar{\nu}_e} = 0.5 \times 10^{51}$ erg s $^{-1}$, the required surface field strengths are 1.4×10^{15} G and 2.9×10^{14} G for $\eta = 3$ and $\eta = 2$, respectively. That B_{crit} decreases as L_ν^{tot} decreases is expected from eq. (18) and the fact that the mass loading of the field lines, \dot{M} , decreases steeply with L_ν^{tot} .

The intersection of P with $\rho v_r^2/2$ (at $r \sim 17$ km) marks the radius of the sonic point and is very well described by eq. (13) for short PNS spin periods, regardless of L_ν^{tot} . Note that for

the B_0 used to plot $B^2/8\pi$ in Fig. 1, for both $\eta = 2$ and $\eta = 3$, that deep in the exponential atmosphere of the PNS, both P and $\rho v_\phi^2/2$ become greater than the magnetic energy density. This is potentially important since we have assumed in constructing these models that corotation obtains ($v_\phi = r\Omega$) everywhere. This assumption is most important between R_ν and R_{sonic} , because centrifugal support in this region can increase \dot{M} significantly. The surface of the PNS calculations, R_ν , is defined as the neutrinosphere (optical depth $\sim 2/3$). This condition determines $\rho(R_\nu)$, which, for most calculations is $\sim 10^{12}$ g cm $^{-3}$. The azimuthal kinetic energy density at R_ν is then determined by setting $\Omega(R_\nu)$. Although in Fig. 1 and §4 we have assumed that R_ν corresponds to the radius at which the magnetic field is anchored ($B(r) = B_0(R_\nu/r)^\eta$), this need not hold necessarily. In addition, very close to the PNS, where the radial flow is very subsonic, we expect the field to be a complex of higher-order multi-poles as shear energy within the PNS convective region emerges as magnetic flux into the magnetically-dominated atmosphere via the Parker instability (Thompson & Murray 2001). The degree of magnetic support within this atmosphere, particularly if differentially rotating, will depend on the dynamics of the underlying convection and the efficacy of the dynamo mechanism, issues that require a multi-dimensional model of these MHD winds.

The importance of the combined action of rapid rotation and strong magnetic fields is seen most clearly in Figure 2. Here, we present the mass loss rate \dot{M} for models with $L_{\bar{\nu}_e} = 8 \times 10^{51}$ erg s $^{-1}$ and 0.5×10^{51} erg s $^{-1}$ as a function of Ω . This range of neutrino luminosity corresponds to roughly 20 seconds of the cooling epoch in the models of Pons et al. (1999). The solid lines assume strict corotation with the PNS surface, $v_\phi = r\Omega$. The dashed lines are presented for comparison assuming no corotation and angular momentum conservation; in these models $v_\phi = R_\nu \Omega(R_\nu/r)$. All mass loss rates quoted are ‘spherical’ and assume $\dot{M} = 4\pi r^2 \rho v_r$. For $\Omega > 3000$ rad s $^{-1}$ in the models assuming corotation, significant deviations from the $\Omega = 0$ limit are obtained. This results from the fact that at this Ω , for $R_\nu = 10$ km, $R_\nu \Omega$ becomes greater than $c_s(R_\nu)$. As alluded to previously (§4), this changes the mass flux in a dramatic way; for $\Omega = 6283$ rad s $^{-1}$ and $L_{\bar{\nu}_e} = 8 \times 10^{51}$ erg s $^{-1}$, $\dot{M} \simeq 8 \times 10^{-3} M_\odot$ s $^{-1}$, more than 30 times larger than in the non-rotating model ($\dot{M} \simeq 2.6 \times 10^{-4} M_\odot$ s $^{-1}$). For comparison, with $\Omega = 9000$ rad s $^{-1}$, $\dot{M} \simeq 0.36 M_\odot$ s $^{-1}$. For $\Omega \gg 3000$ rad s $^{-1}$, the functional dependence of \dot{M} can be approximated roughly with

$$\dot{M}(\Omega R_\nu \gg c_s(R_\nu)) \propto \exp \left[\Omega^2 R_\nu^2 / c_s^2(R_\nu) \right] \quad (28)$$

as expected from simple considerations of the subsonic exponential atmosphere of the PNS. For $\Omega \sim 3000$ rad s $^{-1}$, \dot{M} depends on the location of the sonic point itself (see e.g. Belcher & Macgregor 1976; Hartmann & Macgregor 1982; Lamers & Cassinelli 1999). For rapidly rotating PNSs the spindown timescale may be very short as a result of the large increase in \dot{M} expected when $R_\nu \Omega \gg c_s$ (eqs. 16 and 17). As an example, taking $L_{\bar{\nu}_e} = 8 \times 10^{51}$ erg s $^{-1}$, with $P = 1$ ms, $\eta = 2$, and $B_0 \sim B_{\text{crit}} \sim 3.6 \times 10^{15}$ G, we have from eq. (16) that $\tau_J^R \sim \tau_J^{\text{NR}} \sim 3.1$ seconds. These numbers, together with the scaling relations for τ_J^{NR} and τ_J^R in §4, imply that a significant amount of rotational energy may be extracted from the PNS during the neutrino cooling epoch.

5.3. Rotational Energy Extraction & Spindown

The spindown timescale depends crucially on η . This is seen in eqs. (15) and (22). In addition to the arguments of §3, there are a few things that can be argued with some certainty about the field structure. First, if $B^2/8\pi \ll P$ at the surface, then no closed magnetic field lines will persist and $B_r \propto r^{-2}$, despite the fact that the currents in the star should necessarily produce a dipole field. Although uninteresting from the perspective of spindown because no R_A exists outside R_ν , certainly in this limit we should have $\eta \sim 2$. Second, and at the other extreme, in a totally magnetically dominated system with Γ very large, we expect the field to be dipolar with closed field lines within R_L (although, see §3). In this limit, if we accept the magnetic dipole spindown model for magnetars (and neutron stars generally), then we must have $\eta \sim 3$. These simple arguments suggest that η itself is a function of the ratio of the magnetic flux to the matter flux. Following Ud-Doula & Owocki (2002), one may construct the dimensionless number

$$\xi = B_0^2 R_\nu^2 / \dot{M} v_\infty \quad (29)$$

and write η as a function of ξ . However, with the complications of rapid rotation and relativity, we have decided to simply bracket the possible solution space, computing solutions with $\eta = 2$ and $\eta = 3$ separately as in §4.

Monopole Spindown: We solve the differential equation $I\Omega\dot{\Omega} = \dot{E}_{\text{tot}}$ for $\Omega(t)$ with $\eta = 2$. If $R_A < R_L$ (non-relativistic wind), we use $\dot{E}_{\text{tot}} = -MR_A^2\Omega^2$, with R_A from eq. (9) with $\eta = 2$. If $\Gamma > 1$ (relativistic wind), we take $\dot{E}_{\text{tot}} = \Gamma\dot{M}c^2$, with $\Gamma = B_0^2 R_\nu^4 \Omega^2 M^{-1} c^{-3}$. In order to obtain \dot{M} , we employ the results from our NMC models. We assume that these steady-state wind solutions, for different PNS characteristics, may be concatenated to form a time series. The total neutrino heating rate is computed self-consistently, assuming a PNS neutrino luminosity, including contributions from $\nu_e n \leftrightarrow pe^-$, $\bar{\nu}_e p \leftrightarrow ne^+$, $\nu\bar{\nu} \leftrightarrow e^+e^-$, and inelastic scattering of neutrinos with charged leptons and nucleons (Thompson et al. 2001). For the models presented here, as reflected by the requirement that $R_A\Omega$ is always greater than v_ν (see §4), the total energy deposition rate via neutrino heating and cooling is more than an order of magnitude less $\dot{M}v_\infty^2$. This implies that all wind models are primary driven magnetocentrifugally. In NRNM models of PNS winds, if $\varepsilon_\nu \propto L_\nu^{1/4}$, where ε_ν is the average neutrino energy, $\dot{M} \propto L_\nu^{5/2}$ (Qian & Woosley 1996).¹³ With this dependence in hand from our wind models we need only posit $L_\nu(t)$. Taking $L_\nu(t < 40 \text{ s}) \propto t^{-\alpha}$, with α in the range ~ 1 as appropriate over much of the cooling epoch (see Pons et al. 1999), and $L_\nu(t > 40 \text{ s}) \propto e^{-t/\tau}$ with $\tau = 1$ second, we can compute $\Omega(t)$.

As an example of slow magnetic rotator spindown we take an initial spin period of 20 ms and $B_0 = 1.5 \times 10^{15}$ G. Integrating from $t_i = 1$ s to $t_f = 100$ s, we find that the PNS stops rotating in ~ 50 seconds. In this model a total of $1.75 \times 10^{-4} M_\odot$ is ejected and all of the rotational energy of the PNS is extracted. For this choice of parameters, $\Gamma < 1$ throughout the evolution. For longer spin periods we find similar evolution. The PNS simply stops rotating in tens of seconds. Hence, if magnetars are born slowly rotating (with an initial spin period similar to normal neutron stars) we find that monopolar neutrino-magnetocentrifugal winds can efficiently extract the rotational energy of the young PNS on the Kelvin-Helmholtz timescale.

¹³ This dependence of the mass loss rate on luminosity is only approximate. For very large Ω (above 7000 rad s⁻¹) this power law dependence of \dot{M} on L_ν is modified and the exponent decreases.

As an example of an evolutionary sequence in which we start with a rapidly rotating PNS, we take the initial spin period to be 1 ms and the same temporal evolution of the neutrino luminosity, folding in the exponential dependence of \dot{M} on Ω for $\Omega > 3000$ rad s⁻¹ (as in Fig. 2). Results for $B_0 = 3 \times 10^{15}$ G (A), 1.5×10^{15} G (B), 10^{15} G (C), and 7×10^{14} G (D) are presented in Figure 3. The posited time evolution of L_ν is shown in the lower right panel. The evolution of the mass loss rate follows from the models constructed in §5 and is shown in the upper right panel. Computed evolution of $P(t)$ is in the upper left panel. For clarity of presentation, only the first ~ 20 seconds of $P(t)$ for trajectory (A) are shown. The lower left panel shows the total rotational energy extracted from the PNS as a function of time (solid lines, 10^{51} erg) and the rotational energy loss rate (dashed lines, 10^{51} erg s⁻¹). The lower middle panel shows Γ as a function of t for models (A)–(D), and a model with $B_0 = 1.3 \times 10^{15}$ G (heavy dotted line). Finally, the upper middle panel shows the time evolution of R_L (solid lines) and R_A with $\eta = 2$ (dashed lines).

In model (A) the flow begins with $R_A \sim R_L$. For model (D) several seconds pass before the flow becomes relativistic and Γ becomes greater than 1. For all models shown here, over the 100 seconds of evolution computed, a total of $\gtrsim 2 \times 10^{52}$ erg in rotational energy is lost by the PNS. Because of our assumption of $\eta = 2$, the PNS spin period continues to e -fold on the timescale given by eq. (23). The total mass lost by the PNS decreases as B_0 increases; for model (A) $3.3 \times 10^{-3} M_\odot$ is ejected, whereas for model (D) $5.3 \times 10^{-3} M_\odot$ is emitted. Because Ω drops so rapidly in model (A), and \dot{M} depends exponentially on Ω for $P \lesssim 2$ ms, this correlation is expected. In models (B), (C), and (D), more than 10^{52} erg is emitted with $\Gamma > 100$. In fact, at the end of these spindown calculations, with \dot{M} plummeting with the exponential cutoff in L_ν , Γ can easily reach 1000. The exact evolution depends sensitively on B_0 and the time evolution of \dot{M} , as can be seen from the model with $B_0 = 1.3 \times 10^{15}$ G (dotted line) in the lower middle panel. The complex time evolution of Γ comes both from the exponential cut-off in \dot{M} (imposed at $t = 40$ s) and the fact that Γ can decrease even as the mass loss abates if R_L increases rapidly. That is, for constant B_0 , Γ can decrease if the spindown timescale is shorter than the timescale for \dot{M} to decrease (see eq. 20). The non-relativistic epoch of spindown ($\Gamma < 1$) lasts a mere ~ 1 – 2 s in models (B)–(D), and accounts for ~ 2 – 3×10^{51} erg in rotational energy extracted. Although this timescale is short on the scale of τ_{KH} , it is very long on the scale of the PNS dynamical time and the spin period. Model (A) exhibits begins with near-relativistic flow and only after $t \sim 20$ s does the flow become non-relativistic, with Γ peaking at ~ 100 at $t \sim 6$ seconds. We conclude that spindown in a Weber/Davis-type magnetic field geometry, taking $\eta = 2$, can be significant during the cooling epoch. Even if a monopole-like field structure only obtains during the $\Gamma < 1$ non-relativistic epoch, an amount of energy comparable in magnitude with the supernova explosion itself ($\gtrsim 10^{51}$ erg) is extracted and emerges into the post-explosion supernova ejecta.

Dipole Spindown: We solve for $\Omega(t)$ in the same way as in the monopole case, but here take $\eta = 3$ in calculating R_A and, for $\Gamma > 1$ use $\dot{E}_{\text{tot}} = B_0^2 R_\nu^6 \Omega^4 c^{-3}$. For a *slow* rotator with an initial

period of 20 ms and $B_0 = 10^{15}$ G, the final spin period is ~ 21 ms. That is, a 10^{15} G dipole field does not give significant spindown. For this slow initial rotation period, only a dipole field greater than 10^{16} G affects the evolution significantly before $\Gamma > 1$ and the simple vacuum magnetic dipole limit obtains. As an extreme case, taking $B_0 = 5 \times 10^{16}$ G, the final spin period is ~ 40 ms, more than 70% of the rotational energy is extracted (a mere $\sim 4 \times 10^{49}$ erg), and Γ is greater than unity for $t > 35$ seconds. Figure 4 shows the evolution of $P(t)$, R_L , R_A , Γ , and E and \dot{E} . Virtually all of the braking occurs in these first 35 seconds. As the wind transitions from non-relativistic to relativistic, spindown ceases on the timescale τ_{KH} and the dipole limit obtains.

Figure 5 shows the time evolution computed for PNSs with initial spin period of 1 ms and employing $\eta = 3$. For comparison, the same evolution is shown for three different surface magnetic field strengths, $B_0 = 10^{16}$ G, 5×10^{15} G, and 10^{15} G, labeled ‘A’, ‘B’, and ‘C’, respectively. Panels, linestyles, and units are the same as in Fig. 4. For $B_0 = 10^{15}$ G, the final spin period is 1.15 ms. Although the total change in spin period is small, approximately 10^{51} erg is extracted in the first second of the spindown calculation. A total of $\sim 2 \times 10^{51}$ erg is ejected during the non-relativistic phase of wind evolution ($t \lesssim 9$ s), with $R_A < R_L$ and $\Gamma < 1$. Of course, for the remaining 90 seconds of the spindown calculation, the simple vacuum dipole limit obtains. For higher field strengths the transition from non-relativistic ($\Gamma < 1$) to relativistic ($\Gamma > 1$) occurs at earlier times. For the highest field strength shown here (A), the magnetic energy density dominates the kinetic energy density at R_L throughout the evolution. Most important are our results from the (C) calculation, which show that even taking the more pessimistic dipole field ($\eta = 3$ instead of $\eta = 2$), we find that an amount of energy comparable to the asymptotic supernova energy is naturally injected into the post-shock supernova environment on a short timescale with respect to the amount of time needed for the preceding supernova shockwave to traverse the progenitor (see §6.1).

Note that by decreasing the initial spin period, while keeping $B_0 = 10^{15}$ G, the spindown timescale drops sharply as a result of the exponential dependence of \dot{M} on Ω (see eqs. 9 and 28). For example, taking an initial period of 0.8 ms and $B_0 = 4 \times 10^{15}$ G, one finds $\dot{M} \simeq 0.074 M_\odot \text{ s}^{-1}$ and $R_A \sim 17$ km. This implies a non-relativistic ($\Gamma < 1$; see eq. 17) spindown timescale $\tau_J^{\text{NR}} \sim 2.6$ seconds. For comparison, the vacuum dipole spindown approximation (inappropriate with such large \dot{M}) yields $\tau_J^{\text{R}} \sim 31$ seconds.¹⁴ In the example given, with initial period 0.8 ms and $B_0 = 4 \times 10^{15}$ G only three seconds transpire between the start of the calculation and the moment the vacuum dipole limit obtains. However, in those few seconds, $\sim 10^{52}$ erg is extracted – a total of $0.019 M_\odot$ with velocity $\sim 1.5 - 3 \times 10$ cm s^{-1} . Thus, even in the more pessimistic dipole limit ($\eta = 3$) a significant amount of rotational energy can be extracted on a timescale much shorter than that inferred from a naive and, in this very early phase inappropriate, application of vacuum dipole spindown.

¹⁴ Interestingly, if B_0 is increased, R_A increases, thus decreasing τ_J^{NR} . However, for a given increase in B_0 , τ_J^{R} decreases more than τ_J^{NR} . We find that $\tau_J^{\text{NR}}/\tau_J^{\text{R}} \propto B_0^{(4\eta-6)/(2\eta-1)}$.

¹⁵ Duncan & Thompson (1992) showed that magnetar spindown via vacuum dipole radiation can power hyper-energetic supernovae in Type-II progenitors, but the spindown timescales via this mechanism are not fast enough to explain hyper-energetic Type-Ibc supernovae.

6. DISCUSSION

6.1. Hyper-Energetic Supernovae

For the purposes of this paper we define the word ‘hypernova’ as any supernova with an asymptotic observed total energy of greater than 10^{51} erg. We propose that the magnetically dominated, centrifugally slung winds from rapidly rotating PNSs can explain hypernovae.

In this scenario, core-collapse is followed by shock stall and then explosion. The explosion may be caused by a combination of neutrino heating and convection (e.g. Herant et al. 1994; Burrows, Hayes, & Fryxell 1995; Fryer & Warren 2002), by neutrino heating plus rotation and dissipative effects (Thompson, Quataert, & Burrows in prep) or perhaps via MHD-driven jets (Akiyama et al. 2003). In any case, the supernova shock propagates outward at $\sim 10,000$ km s^{-1} with energy $\sim 10^{51}$ erg. The wind phase commences as the PNS contracts and cools. In the first few seconds, the kinetic energy density and thermal pressure of the wind are large and the wind is not magnetically dominated. The wind hydrodynamical power in this phase is inefficiently supplied by neutrino heating as in NRNM wind models. As the radius of the PNS decreases, the average magnetic field grows because of flux conservation ($B_0 \propto R_\nu^{-2}$) and an efficient dynamo as in Duncan & Thompson (1992). The PNS also spins up as a result of angular momentum conservation. The hydrodynamical power of the wind decreases with the neutrino luminosity and there is a point in time when the magnetic energy density begins to dominate the thermal and kinetic wind energy density. An Alfvén point will form, and efficient extraction of the rotational energy from the PNS will commence. The mass loss rate will likely *increase* in this phase despite the decrease in the neutrino luminosity as R_A approaches R_{sonic} , assuming that $R_\nu \Omega$ exceeds $c_s(R_\nu)$ (see §5). This is a result of the exponential dependence of \dot{M} on Ω^2 in the centrifugal limit. For a rapidly rotating PNS, our calculations show that for η close to 2, of order 10^{52} erg is naturally extracted in the first few seconds. In §5.3 we showed that even in the case $\eta = 3$, by appealing to slightly higher B_0 and Ω , of order 10^{52} erg can be extracted on a few-second timescale. The velocity of this wind material evolves quickly to near c and the NMC wind drives a secondary shock into the post-supernova-shock material. This secondary, but much more energetic shock encounters the slower supernova shock while still inside the progenitor of a Type-II or Type-Ibc supernova (probably at a radius $\lesssim 10^5$ km).¹⁵ In this way, a hyper-energetic supernova is created.

Only in a very compact progenitor will the secondary wind shock collide with the preceding supernova shock outside the star. This could plausibly occur in accretion-induced collapse of a white dwarf. Otherwise, we expect this very energetic shock to alter the nucleosynthetic signature of the hypernova with respect to normal supernovae, producing excess nickel as inferred from, e.g. SN1998bw and SN2003dh (Nakamura et al. 2001a,b; Maeda et al. 2003; Woosley & Heger 2003). If magnetars are born in progenitors with extended envelopes, these strong magnetocentrifugal outflows might also prevent late-time fallback accretion (Chevalier 1989; Woosley

& Weaver 1995; Fryer et al. 1996). Although the simple analysis presented here assumes sphericity, because the outflow is magnetocentrifugally driven, we expect asymmetries in the ejecta due to collimation (e.g. Sakurai 1985; Begelman & Li 1994).

6.2. Gamma Ray Bursts

Although the time evolution is complex and depends sensitively on B_0 , our models generally achieve large Γ as \dot{M} decreases at R_L (see middle lower panel in Fig. 3). Even though the velocity of the matter at R_L is only mildly relativistic, asymptotically the energy of the field may be transferred to the wind material, yielding ultra-relativistic velocities. If all of the magnetic energy at R_L is eventually converted to kinetic energy, the asymptotic limiting Lorentz factor (γ_∞) of the matter is Γ , given by eq. (20).¹⁶ Our exploration of the spindown of PNSs with 1 ms initial periods shows that Γ may be very large with \dot{E} in the range $\gtrsim 10^{51}$ erg s⁻¹. In fact, we obtain of order $\sim 10^{51} - 10^{52}$ erg emitted on a 10–100 second timescale with $\Gamma \gtrsim 100$ (Fig. 3). This conclusion is particularly robust for the optimistic monopole-like field geometry with $\eta = 2$. The correspondence between the energy budget, energy loss rates, and Lorentz factors inferred from observations of GRBs and the models presented here support the conclusion that a class of PNSs, born highly magnetic and rapidly rotating within compact progenitors, may be responsible for cosmological gamma ray bursts (Usov 1992; Thompson 1994).

The now-robust association of long-duration GRBs with highly energetic supernovae, as evidenced by SN1998bw (Galama et al. 1998) and SN2003dh (Stanek et al. 2003; Hjorth et al. 2003), follows naturally from our discussion of hypernovae in §6.1. As described in §6.1, we can expect complex shock structure evolution as the energy loss rate changes and the outflow becomes increasingly more relativistic. The dynamics of the supernova-shock/wind-shock interaction with the envelope and the associated instabilities might be important both in producing internal shocks and time variability and ultra-high-energy cosmic rays (Arons 2003). There are other ways to produce time variability. We find that large changes in Γ naturally occur as R_L evolves with Ω (see Fig. 3). This order unity variability in Γ provides a mechanism for producing internal shocks (Thompson 1994; Rees & Mészáros 1994). Shocks in the flow can also be created by fluctuations in mass loading caused by sudden changes in \dot{M} . Closed loops that trap wind material on the surface of the PNS may be sheared open on millisecond timescales due to convection or differential rotation or may be opened by continued neutrino heating of the trapped matter (Thompson 2003). Finally, relativistic MHD instabilities (e.g. reconnection) may produce time-variability in Poynting-flux dominated outflows.

The duration of gamma ray bursts in the magnetar model presented here is somewhat uncertain and could be set by either the spindown time of the PNS (τ_J) or the PNS cooling time τ_{KH} .¹⁷ The latter would be appropriate if $\tau_J > \tau_{\text{KH}}$ and if the magnetic field significantly decreases after the cooling epoch, leading to a decrease in wind luminosity and thus an

end to a detectable GRB. The field at the Alfvén point (relevant for the spindown power) could decrease either because the *surface* field decreases in strength as convection in the PNS ceases (Thompson 1994) or because the field may transition from monopole-like to dipole-like as \dot{M} decreases.

A further important feature of the magnetar model presented here is that in the monopole case, \dot{E} decreases *exponentially* as a function of t with timescale given by eq. (23). This is a prediction of the monopole-like magnetar model and it stands in sharp contrast to the energy loss rate predicted from both collapsar-type models (Woosley 1993) whose \dot{E} must evolve on the timescale for accretion onto the central compact object. Equation (23) also shows that if the field is increased to 10^{16} G that $\tau_J^{\text{R}} \sim 0.3$ seconds, which is in the middle of the distribution for short-duration GRBs. Similarly, allowing for lower B_0 and Ω , we further speculate that if magnetars are responsible for long-duration GRBs, that much longer ($\gtrsim 1000$ s) GRBs may exist and could be detected by upcoming observations with improved sensitivity (e.g. SWIFT). If one allows for a dynamo mechanism operating efficiently within the convective core of protoneutron stars (Duncan & Thompson 1992; Thompson & Duncan 1993) then B_0 is directly proportional to Ω to some power, depending on the details of the dynamo. If there is such a relationship between B_0 and Ω , then the diversity of GRB sources, both long and short GRBs (Kouveliotou et al. 1993) as well as hyper-energetic supernovae, may be grouped in a one-parameter family, a function only of rotation period. In this way, the birth of rapidly rotating PNSs may be responsible for a diverse variety of astrophysical explosions. We speculate that short bursts come from more rapidly rotating progenitors with no extended envelope. For example, the short GRB population may be due to accretion-induced collapse of a white dwarf (leading to a sub-millisecond PNS), whereas the long population is from collapse of Type-Ibc progenitors (perhaps only ~ 1 ms periods). Another possibility for short GRBs is that the merger of a neutron star binary creates a black hole or massive rapidly rotating neutron star that drives a wind similar to those detailed in this paper (Thompson 1994). The scaling relations derived here are applicable in this context as well for magnetocentrifugally driven flows off the accretion torus produced from the inner regions of a black hole accretion disk. In either case, the short bursts would trace an old stellar population, whereas the long bursts would be associated with star-forming regions.

That the birth of neutron stars with magnetar-like field strengths might be the astrophysical origin of GRBs is not new. The idea presented here follows that of Usov (1992) and Thompson (1994) and touches on any model of GRBs requiring Poynting-flux dominated outflows (e.g. Lyutikov & Blandford 2003). In Usov (1992) and Thompson (1994), only a pure dipole field geometry was considered. In this paper we find potentially much larger energy loss rates for a given B_0 and Ω as a consequence of different field geometries. In particular, motivated by the literature on stellar winds and their angular momentum evolution, we have considered monopole field topologies in the spirit of Weber & Davis (1967). Further consideration of rapid rotation coupled with high mass loss rates (see §3; Mestel & Spruit 1987) supports this view. The energy extraction rates and braking suggested by our pure monopole calcu-

¹⁶ Analyses of ideal relativistic winds predict that $\gamma_\infty \sim \Gamma^{1/3}$ (Michel 1969; Goldreich & Julian 1970; Beskin et al. 1998). However, modeling of the equatorial relativistic wind of the Crab pulsar (Kennel & Coroniti 1984a,b; Spitkovsky & Arons 2003) suggests that $\gamma_\infty \sim \Gamma$ and *not* that $\gamma_\infty \sim \Gamma^{1/3}$, in contradiction with theoretical expectations.

¹⁷ In principle the duration could also be set by much more ‘messy’ physics such as the detailed emission model and how it depends on \dot{E} and Γ in the wind.

lations (see §4 and §5.3) are likely overly optimistic. However, we await multi-dimensional MHD models of relativistic outflows.

In addition to the issue of field topology there are other important potential difficulties inherent to this GRB mechanism. Similar to the collapsar model of GRBs (Woosley 1993; Macfadyen & Woosley 1999), the energy injection rate must remain high on the timescale of the relativistic ejecta to break out of the progenitor. Given the timescales we have derived and τ_{KH} , this is plausible for compact Type-Ibc core-collapse scenarios. In addition, we rely on conversion of magnetic energy into kinetic energy asymptotically, a process that is not well understood in models of pulsar winds. Issues of collimation and – possibly – jet formation require multi-dimensional models and we assume that many of the structures generic to collapsar jets will obtain here as well (Aloy et al. 2000; Zhang et al. 2003), although the flow will be Poynting-flux dominated.

6.3. Conclusions

We have estimated spindown timescales for protoneutron stars born rapidly rotating and with large surface magnetic field strengths. The combination of magnetocentrifugal effects and neutrino energy deposition combine to produce a wind capable of significantly effecting the early angular momentum evolution of newly born protoneutron stars. In addition, we have constructed steady-state models of neutrino-magnetocentrifugal winds, including magnetic fields implicitly and approximately by forcing the wind matter into strict corotation with the PNS.

We find that magnetar-like surface fields ($\sim 10^{15}$ G) dominate the thermal pressure and kinetic energy density of PNS winds in the first few seconds after the preceding supernova for a wide range of initial spin periods. We show that as the mass loss from the PNS abates, the outflow becomes increasingly faster, transitioning from non-relativistic to relativistic outflow in the first few to tens of seconds. We explore this progression and provide evolutionary models that bridge the transition. We find that non-relativistic spindown timescales can be considerably shorter than those inferred from simple vacuum dipole spindown. This results both from physics of the Alfvén point and the large enhancement in mass loss rate expected in models with spin periods less than ~ 2 ms (see §5 and Fig. 2). Motivated by the literature on stellar winds from magnetic rotating stars, we have carried out calculations for monopole-like field geometries in addition to pure dipole fields (see §3 and §5). Although optimistic in computing spindown, quasi-monopolar fields are physically motivated by the large mass loss and rapid rotation of the systems considered. We are currently working on axi-symmetric two-dimensional MHD models to more fully explore the issue of global magnetic field topology and angular momentum loss.

Regardless of field topology, we find generically in our models that if magnetars are born with ~ 1 ms initial periods and $B_0 \sim 10^{15}$ G that more than 10^{51} erg of rotational energy can be extracted in the first few seconds and that the velocity of this matter will approach c as the Alfvén radius approaches the light cylinder. As the mass loss rate continues to plummet, the asymptotic limiting Lorentz factor of the ejected matter may approach several hundred. We therefore propose these objects as candidate central engines for hyper-energetic supernovae and cosmological gamma ray bursts of both the long and, possibly, the short variety (see also Usov 1992, Thompson 1994, and Lyutikov & Blandford 2003).

Although more mundane from an energetic point of view, if monopolar field geometries are at all relevant for slow rotators ($P \gtrsim 20$ ms), efficient angular momentum loss results. We find that if magnetars are born with the spin periods of normal neutron stars, taking $\eta = 2$, that a PNS can be spun down from a spin period of ~ 50 ms to a spin period of ~ 1 second in ~ 10 seconds of wind evolution.

We emphasize that for any field strength there is a point in time during the cooling of the nascent neutron star when the magnetic field dominates the wind dynamics. If the field is strong enough, this happens early in the wind phase and efficient extraction of rotational energy is likely a natural consequence. The neutrinos still carry away the neutron star’s binding energy ($\sim 3 \times 10^{53}$ erg), but their energetic coupling with the surrounding environment is (necessarily) weak. In marked contrast, the rotational energy (although only of order 10^{52} erg for a fast rotator) may be efficiently coupled to the wind material via the strong magnetic field. It is in this way that the wind’s energetic presence within supernova remnants and in the spin distribution of neutron stars may be observed.

We thank Lars Bildsten for originally suggesting this problem and for helpful conversations on potential observational implications. We gratefully acknowledge conversations with Jonathan Arons, Anatoly Spitkovsky, Yoram Lithwick, Brian Metzger, and Adam Burrows. We are also indebted to Chris Thompson and Henk Spruit for a critical reading of the text and for helpful comments and suggestions for improvement. We thank Evonne Marietta for making her general electron-positron EOS available. T.A.T. thanks the Aspen Center for Physics, where much of this work germinated. T.A.T. is supported by NASA through Hubble Fellowship grant #HST-HF-01157.01-A awarded by the Space Telescope Science Institute, which is operated by the Association of Universities for Research in Astronomy, Inc., for NASA, under contract NAS 5-26555. E.Q. is supported in part by NSF grant AST 0206006, NASA grant NAG5-12043, an Alfred P. Sloan Fellowship, the David and Lucile Packard Foundation, and a Hellman Faculty Fund Award.

REFERENCES

- Akiyama, S., Wheeler, J. C., Meier, D., & Lichtenstadt, I. 2003, *ApJ*, 584, 954
Aloy, M.-A., Müller, E., Ibáñez, J., Martí, J., MacFadyen, A. 2000, *ApJL*, 531, L119
Arons, J. 2003, *ApJ*, 589, 871
Arras, P. & Lai, D. 1999, *PRD*, 60, 043001
Begelman, M. C. & Li, Z.-Y. 1994, *ApJ*, 426, 269
Belcher, J. W. & Macgregor, K. B. 1976, *ApJ*, 210, 498
Beskin, V. S., Kuznetsova, I. V., & Rafikov, R. R. 1998, *MNRAS*, 299, 341
Burrows, A., Hayes, J., & Fryxell, B. A. 1995, *ApJ*, 450, 830
Burrows, A. & Lattimer, J. M. 1986, *ApJ*, 307, 178
Cardall, C. Y. & Fuller, G. M. 1997, *ApJL*, 486, 111
Chevalier, R. 1989, *ApJ*, 346, 847
Duncan, R. C., Shapiro, S. L., & Wasserman, I. 1986, *ApJ*, 309, 141
Duncan, R. C. & Thompson, C. 1992, *ApJL*, 392, 9
Fryer, C., Benz, W., & Herant, M. *ApJ*, 460, 801
Fryer, C. & Warren, M. 2002, *ApJL*, 574, L65

- Galama, T. J., et al. 1998, *Nature*, 395, 670
- Goldreich, P. & Julian, W. H. 1970, *ApJ*, 160, 971
- Gunn, J. E. & Ostriker, J. P. 1969, *Nature*, 221, 454
- Harding, A., Contopolous, I., & Kazanas, D. 1999, *ApJL*, 525, L125
- Hartmann, L. & Macgregor, K. B. 1982, *ApJ*, 259, 180
- Herant, M., Benz, W., Hix, W. R., Fryer, C., & Colgate, S. 1994, *ApJ*, 435, 339
- Hjorth, J., et al. 2003, *Nature*, 423, 847
- Keil, W., Janka, H.-Th., & Müller, E. 1996, *ApJL*, 473, L111
- Kennel, C. F. & Coroniti, F. V. 1984a, *ApJ*, 283, 694
- Kennel, C. F. & Coroniti, F. V. 1984b, *ApJ*, 283, 710
- Keppens, R. & Goedbloed, J. P. 1999, *A&A*, 343, 251
- Kouveliotou, C., Meegan, C., Fishman, G., Bhat, N., Briggs, M., Koshut, T., Paciasas, W., & Pendelton, G. 1993, *ApJL*, 413, L101
- Kouveliotou, C., Strohmayer, T., Hurley, K., van Paradijs, J., Finger, M. H., Dieters, S., Woods, P., Thompson, C., Duncan, R. C. 1999, *ApJL*, 510, 115
- Lai, D. & Qian, Y.-Z. 1998, *ApJ*, 505, 844
- Lamers, H. & Cassinelli, J. P., *Introduction to Stellar Winds* (Cambridge University Press, Cambridge, 1999)
- Lionello, R., Linker, J. A., & Mikic, Z. 2001, *ApJ*, 546, 542
- Lyutikov, M. & Blandford, R. 2003, *astro-ph/0312347*
- Maeda, K., Mazzali, P. A., Deng, J., Nomoto, K., Yoshii, Y., Tomita, H., & Kobayashi, Y. 2003, *ApJ*, 593, 931
- MacFadyen, A. I. & Woosley, S. E. 1999, *ApJ*, 524, 262
- Mestel, L. 1968, *MNRAS*, 138, 359
- Mestel, L. & Spruit, H. C. 1987, *MNRAS*, 226, 57
- Michel, F. C. 1969, *ApJ*, 158, 727
- Nakamura, T., Mazzali, P., Nomoto, K., Iwamoto, K. 2001a, *ApJ*, 550, 991
- Nakamura, T., Umeda, H., Iwamoto, K., Nomoto, K., Hashimoto, M., Hix, W. R., & Thielemann, F.-K. 2001b, *ApJ*, 555, 880
- Ostriker, J. P. & Gunn, J. E. 1969, *ApJ*, 157, 1395
- Otsuki, K., Tagoshi, H., Kajino, T., & Wanajo, S.-Y. 2000, *ApJ*, 533, 424
- Pacini, F. 1967, *Nature*, 216, 567
- Pacini, F. 1968, *Nature*, 219, 145
- Pizzo, V., Schwenn, R., Marsch, E., Rosenbauer, H., Mülhåuser, K.-H., & Neubauer, F. M. 1983, *ApJ*, 271, 335
- Pneuman, G. W. & Kopp, R. A. 1971, 18, 258
- Poe, C. H., Friend, D. B., & Cassinelli, J. P. 1989, *ApJ*, 337, 888
- Pons, J. A., Reddy, S., Prakash, M., Lattimer, J. M., & Miralles, J. A. 1999, *ApJ*, 513, 780
- Qian, Y.-Z. & Woosley, S. E. 1996, *ApJ*, 471, 331
- Rees, M. & Mészáros P. 1994, *ApJL*, 430, 93
- Sakurai, T. 1985, *A&A*, 152, 121
- Schatzman, E. 1962, *Annales d'Astrophysique*, 25, 18
- Spitkovsky, A. & Arons, J. 2003, *ApJ*, in press
- Stanek, K. Z., et al. 2003, *ApJL*, 591, L17
- Steinolfson, R. S., Suess, S. T., & Wu, S. T. 1982, *ApJ*, 255, 730
- Sumiyoshi, K., Suzuki, H., Otsuki, K., Teresawa, M., & Yamada, S. 2000, *PASJ*, 52, 601
- Taam, R. E. & Spruit, H. C. 1989, *ApJ*, 345, 972
- Takahashi, K., Witt, J., & Janka, H.-T. 1994, *A&A*, 286, 857
- Thompson, T. A., Burrows, A., & Meyer, B. S. 2001, *ApJ*, 562, 887
- Thompson, T. A. 2003a, *ApJL*, 585, L33
- Thompson, T. A. 2003b, *Core-Collapse of Massive Stars*, Edited by C. Fryer, Kluwer Academic Publishers
- Thompson, C. 1994, *MNRAS*, 270, 480
- Thompson, C. & Duncan, R. C. 1993, *ApJ*, 408, 194
- Thompson, C. & Blaes, O. 1998, *PRD*, 57, 3219
- Thompson, C. & Murray, N. 2001, *ApJ*, 560, 339
- Thompson, C., Lyutikov, M., & Kulkarni, S. R. 2002, *ApJ*, 574, 332
- Ud-Doula, A. & Owocki, S. P. 2002, *ApJ*, 576, 413
- Ud-Doula, A. 2002, Ph.D. Thesis, University of Delaware
- Usov, V. 1992, *Nature*, 357, 472
- Usmanov, A., Goldstein, M., Besser, B., & Fritzer, J. 2000, *J. Geophys. Res.*, 105, 12675
- Van der Holst, B., Banerjee, D., Keppens, R., & Poedts, S. 2002, Proc. 10th European Solar Physics Meeting, *Solar Variability: From Core to Outer Frontiers*, Prague, Czech Republic, Ed. A. Wilson, p.75
- Villain, L., Pons, J., Cerda-Duran, P., Gourgoulhon, E. 2003, *astro-ph/0310875*
- Wanajo, S., Kajino, T., Mathews, G. J., & Otsuki, K. 2001, *ApJ*, 554, 578
- Weber, E. J. & Davis, L. 1967, *ApJ*, 148, 217
- Woosley, S. E. 1993, *ApJ*, 405, 273
- Woosley, S. E., Wilson, J. R., Mathews G. J., Hoffman, R. D., & Meyer, B. S. 1994, *ApJ*, 433, 209
- Woosley, S. E. & Weaver, T. A. 1995, *ApJS*, 101, 181
- Woosley, S. E. & Heger, A. 2003, submitted to *ApJ*, *astro-ph/0301965*
- Yuan, Y. & Heyl, J. 2003, *astro-ph/0305083*
- Zhang, W., Woosley, S. E., & MacFadyen, A. I. 2003, *ApJ*, 586, 356

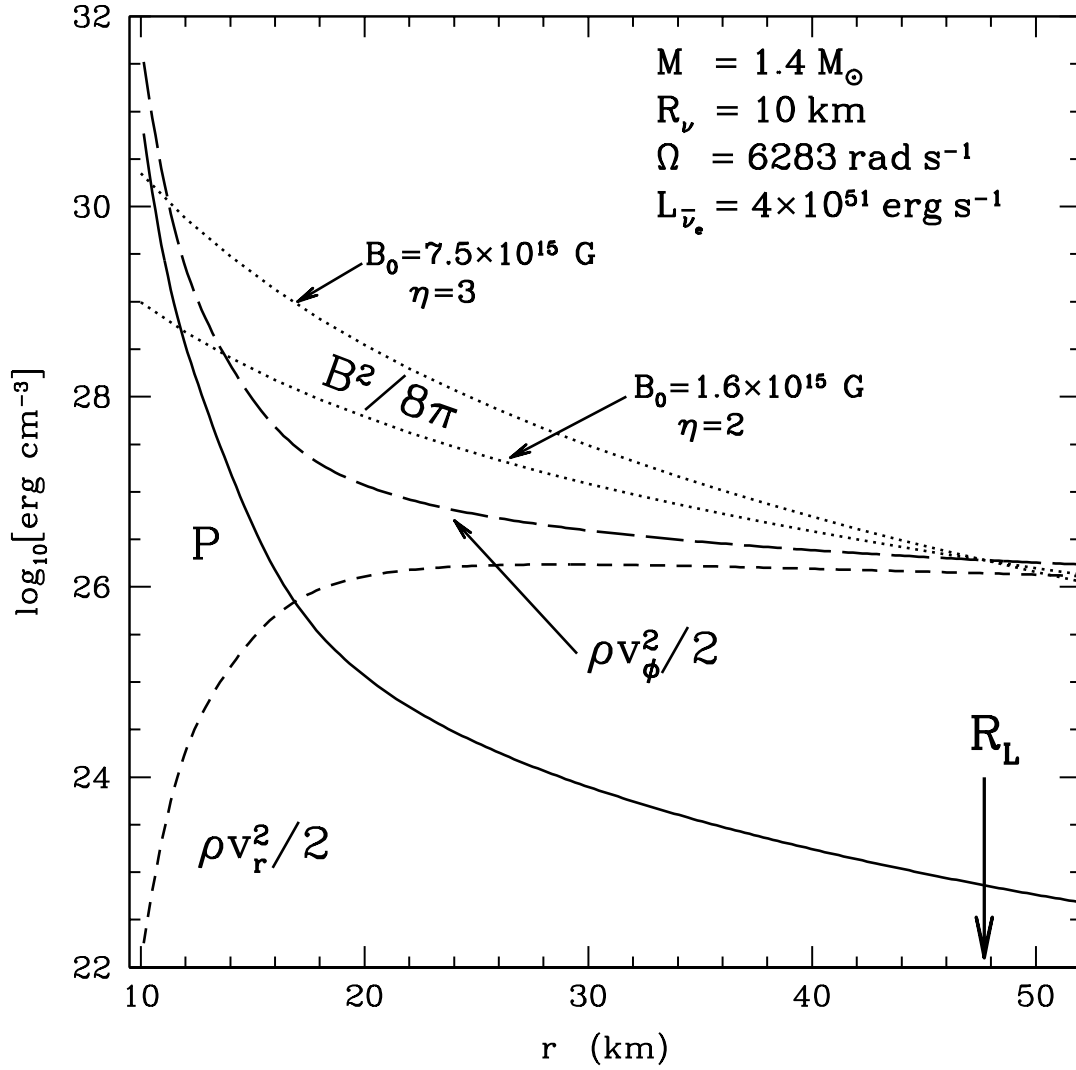


FIG. 1.— Thermal pressure (P , solid line), kinetic energy density ($\rho v_r^2/2$, short dashed line; $\rho v_{\phi}^2/2$, long dashed line), and magnetic energy density ($B^2/8\pi$, dotted lines) for $B_0 = 1.6 \times 10^{15} \text{ G}$ and $B_0 = 7.5 \times 10^{15} \text{ G}$ for $\eta = 2$ and $\eta = 3$, respectively, as a function of radius. The PNS has spin period of 1 ms ($\Omega \simeq 6283 \text{ rad s}^{-1}$, $R_L \simeq 47.7 \text{ km}$ is the corresponding light cylinder radius), $L_{\bar{\nu}_e} = 4 \times 10^{51} \text{ erg}$, $R_{\nu} = 10 \text{ km}$, and $M = 1.4 M_{\odot}$. The mass loss rate is $\dot{M} \simeq 1.6 \times 10^{-3} M_{\odot} \text{ s}^{-1}$ (compare with Fig. 2). Model numbers were chosen to closely follow those employed for the scaling relations in §4.

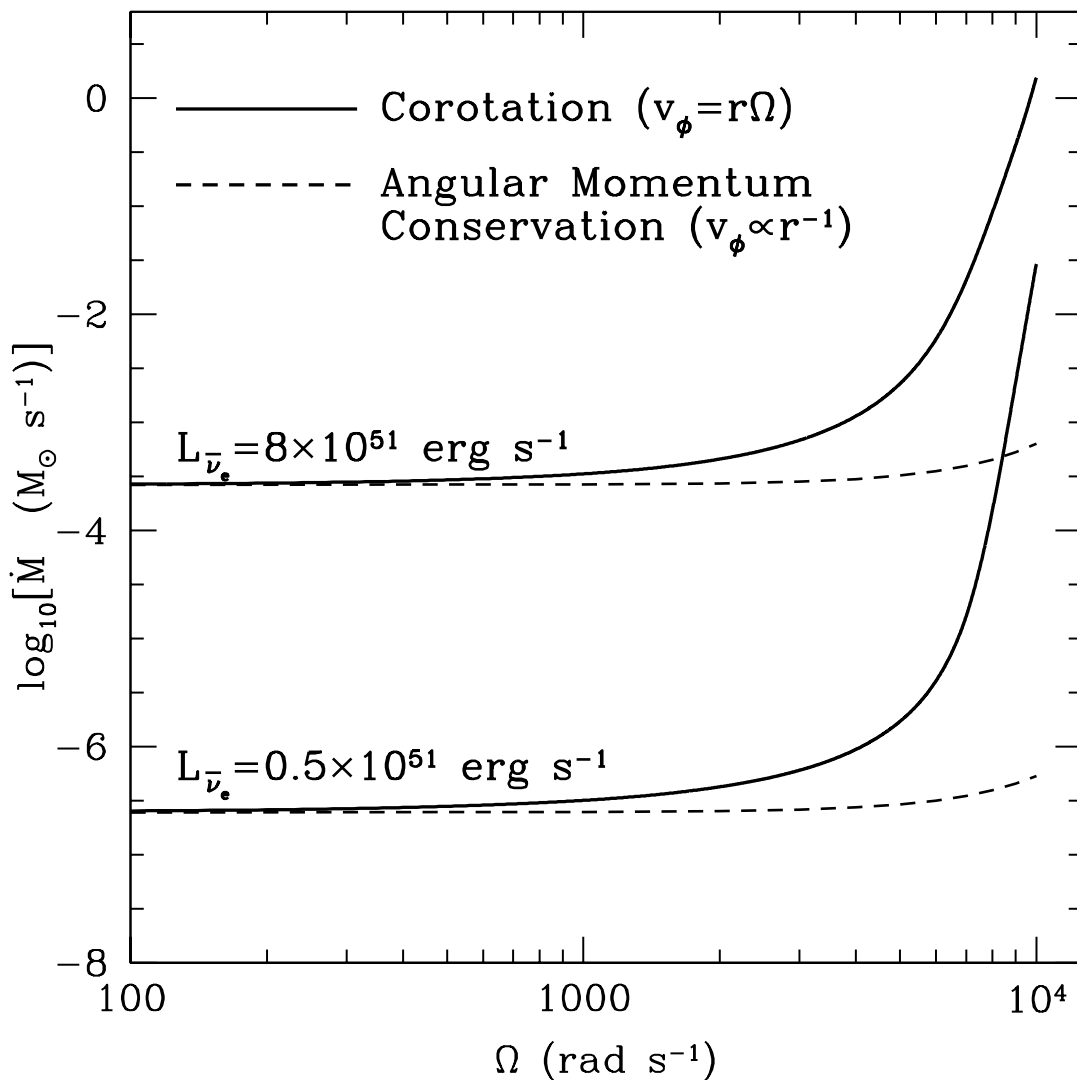


FIG. 2.— Log of the mass loss rate as a function of Ω for $L_{\bar{\nu}_e} = 8 \times 10^{51} \text{ erg s}^{-1}$ and $L_{\bar{\nu}_e} = 0.5 \times 10^{51} \text{ erg s}^{-1}$ assuming corotation with the PNS surface, $v_{\phi} = r\Omega$ (solid lines). Also shown are results assuming no corotation (dashed lines), but taking $v_{\phi} = R_{\nu}\Omega(R_{\nu}/r)$, appropriate for angular momentum conservation. For $R_{\nu}\Omega > c_s(R_{\nu})$, \dot{M} increases approximately exponentially with Ω^2 in the models assuming corotation.

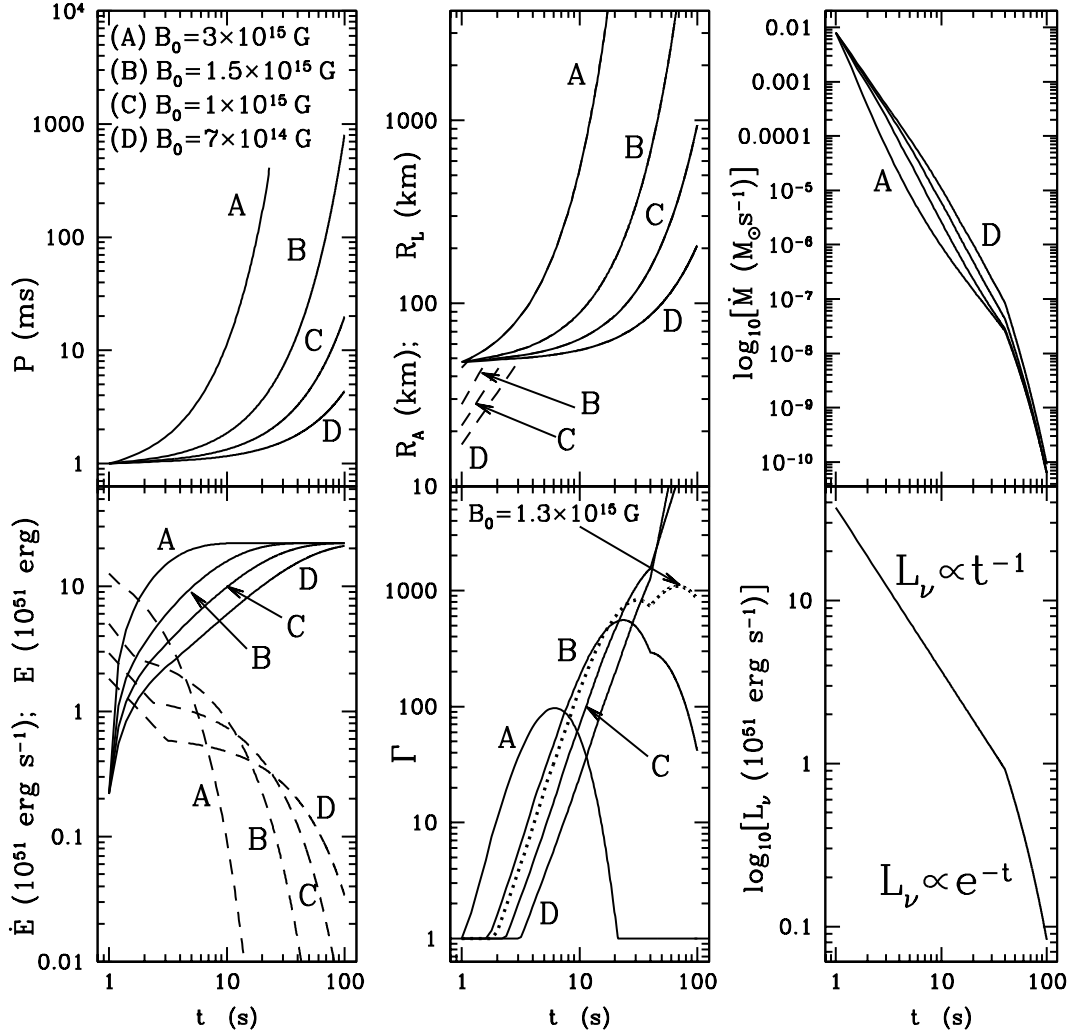


FIG. 3.— Representative time evolution for the spin evolution of a rapidly rotating highly magnetic PNS with a monopole field geometry ($\eta = 2$). Calculations with four different surface magnetic field strengths are shown: $B_0 = 3 \times 10^{15}$ G (A), 1.5×10^{15} G (B), 10^{15} G (C), and 7×10^{14} G (D). The upper and lower right panels show the mass loss rate (\dot{M} [$M_\odot s^{-1}$]) and the total neutrino luminosity ($\log_{10} L_\nu$ [10^{51} erg s^{-1}]), respectively. The spin period (P [ms]; upper left panel), limiting asymptotic Lorentz factor (Γ ; lower middle panel), spin energy extracted (E [10^{51} erg]; lower left panel, solid lines), and energy extraction rate (\dot{E} [10^{51} erg s^{-1}]; lower left panel, dashed lines), are shown. In addition, the upper-middle panel shows R_L (solid lines) and R_A as computed with $\eta = 2$ (dashed lines). For comparison, in the plot of Γ versus t , we also include the evolution for $B_0 = 1.3 \times 10^{15}$ G (dotted line), which falls between models (B) and (C). Note the interesting time evolution of Γ as \dot{M} drops exponentially after $t = 40$ s, in response to the assumed change in L_ν .

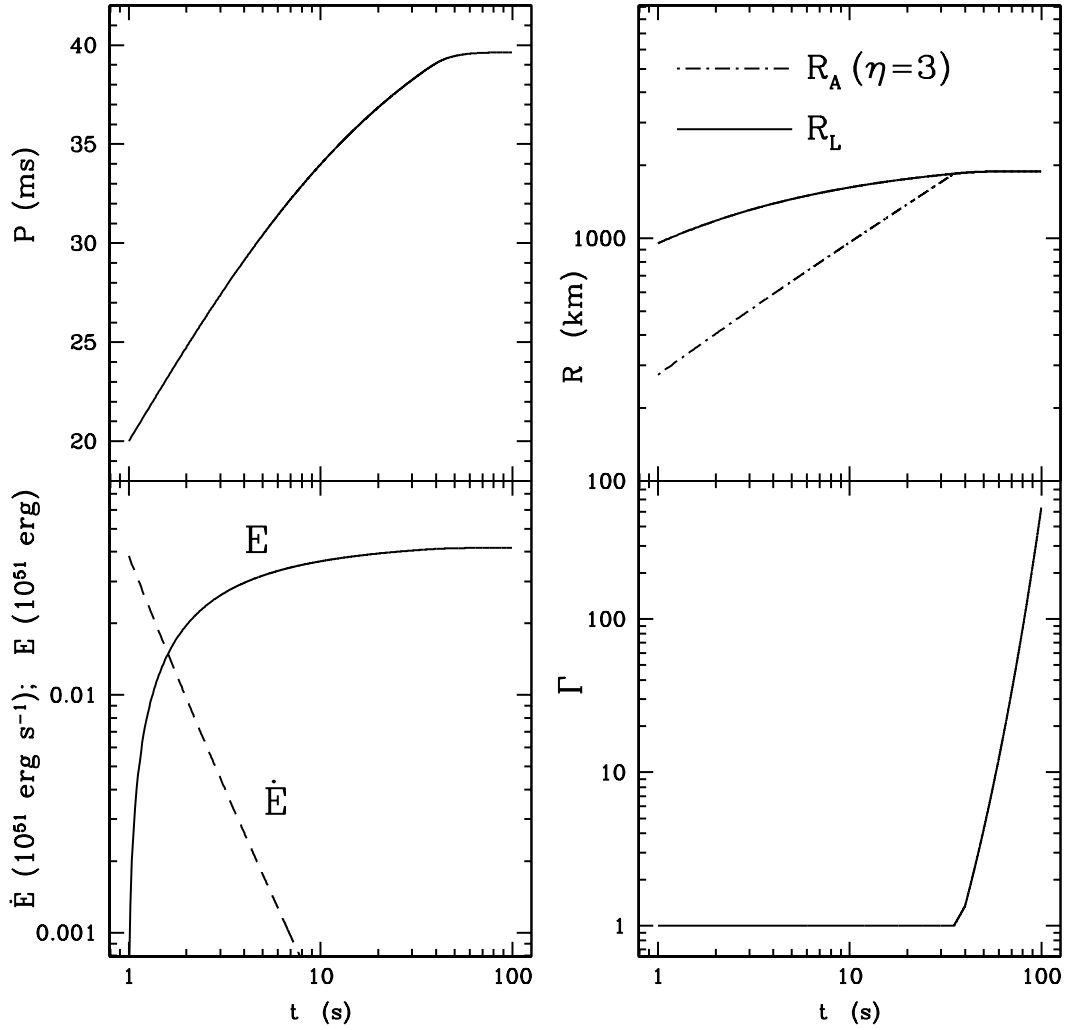


FIG. 4.— Representative time evolution for the spin evolution of a slowly rotating highly magnetic PNS with a dipole field geometry ($\eta = 3$). Spin period (P [ms]; upper left panel), limiting asymptotic Lorentz factor (Γ ; lower right panel), light cylinder radius (R_L [km], upper right panel, solid line), Alfvén radius (R_A [km], upper right panel, dot-dashed line), spin energy extracted (E [10^{51} erg]; lower left panel, solid line), and energy extraction rate (\dot{E} [10^{51} erg s^{-1}]; lower left panel, dashed line), are shown. As an extreme example, B_0 was taken to be 5×10^{16} G.

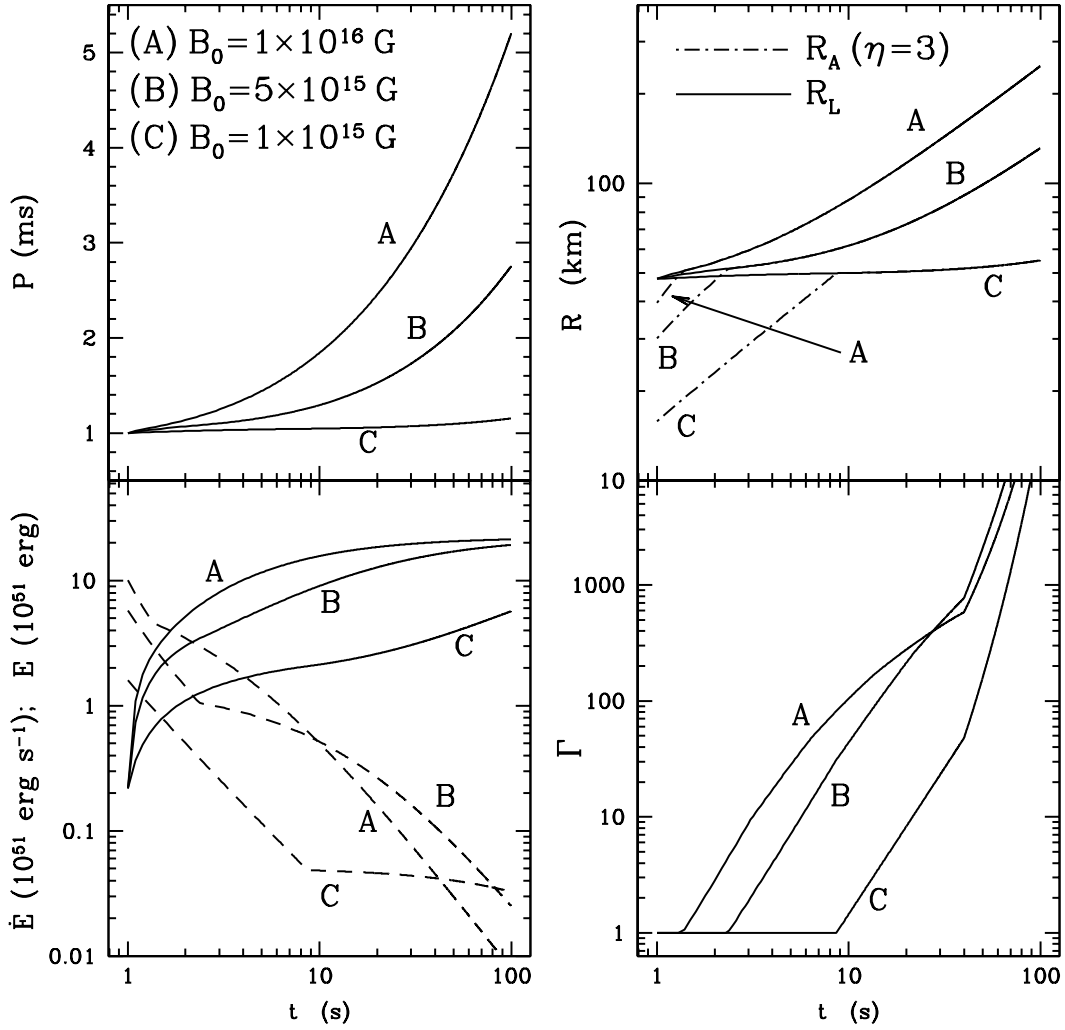


FIG. 5.— Representative time evolution for the spin evolution of a rapidly rotating highly magnetic PNS with a dipole field geometry ($\eta = 3$). Calculations with three different surface magnetic field strengths are shown: $B_0 = 10^{16}$ G (A), 5×10^{15} G (B), and 10^{15} G (C). Panels, units, and linestyles are the same as in Fig. 4.